International Journal of Basic and Applied Sciences, 14 (8) (2025) 136-141

International Journal of Basic and Applied Sciences

Website: www.sciencepubco.com/index.php/IJBAS
https://doi.org/10.14419/bwb02d23
Research paper

Enhanced Black Ice Detection in Road Environments Using LiDAR and Angle-Thermal Modulation

Seung-Beom Hong, Won-hyuk Choi *

Department of Avionics, Hanseo University
**Corresponding author E-mail: choiwh@hanseo.ac.kr*

Received: September 24, 2025, Accepted: November 10, 2025, Published: December 4, 2025

Abstract

This paper explores a LiDAR-based approach for identifying black ice on road surfaces by analyzing variations in distance measurements under controlled changes in temperature and sensor orientation. Utilizing the compact and economical Lidar Lite v3, we observed how sub-tle differences in reflectivity and surface angle can distinguish black ice from asphalt. Despite the sensor's ±1 cm error margin, experimental outcomes suggest it is feasible to detect black ice through this method. The proposed approach offers a potential solution for real-time road hazard monitoring and sets the foundation for further enhancements aimed at improving robustness in dynamic environments.

Keywords: *Black Ice Detection; LiDAR Lite v3 Sensor; Surface Reflectivity Analysis.*

1. Introduction

Black ice, an almost invisible layer of frozen moisture on road surfaces, poses a serious threat to driving safety, especially during winter when drivers cannot easily recognize it. Conventional detection systems often rely on thermal cameras or embedded sensors, which can be costly, complex to install, or prone to interference from environmental factors. To overcome these limitations, this study proposes a lightweight and non-intrusive method for identifying black ice using laser-based distance measurements. The method utilizes the Lidar Lite v3 sensor, a compact and affordable device capable of measuring distance with sufficient accuracy for surface condition analysis. By adjusting the sensor's tilt angle and observing surface temperature changes, we analyze how the reflective properties of asphalt and black ice differ in measurable ways. This enables detection based not on visual or thermal cues, but on the behavior of laser reflection under controlled conditions. Preliminary results show that while temperature alone does not provide reliable discrimination due to the sensor's insensitivity to thermal variation, angular measurements yield more distinguishable patterns between frozen and non-frozen surfaces. These findings support the development of real-time black ice detection systems that can be integrated into road safety infrastructure or advanced driver assistance platforms.

2. LiDAR-Based Black Ice Detection Approach

2.1. Limitations of conventional black ice detection methods

Figure 1 illustrates a hazardous road condition where a surface has become dangerously slippery due to the formation of black ice. In such situations, conventional visual cues are often insufficient, as black ice is nearly transparent and blends seamlessly with asphalt, making it extremely difficult for both human observers and traditional optical systems to identify. To address these challenges, previous studies have explored diverse sensor-based and optical approaches. For instance, BlackIceNet [2] proposed an explainable AI framework that integrates multimodal data – combining LiDAR intensity, thermal imagery, and environmental parameters – to enhance detection under low-visibility conditions. While these systems are effective, they rely on complex sensor fusion architectures and high computational resources, which limit their scalability in distributed roadside environments. In a similar vein, Ma and Ruan [13] employed tri-wavelength backscattering measurements to enhance the accuracy of black-ice recognition on road surfaces. However, this approach requires specialised multi-wavelength LiDAR hardware, which is costly and not suitable for large-scale deployment. In contrast, the method proposed in this study focuses on angular reflectance profiling using a single, low-cost LiDAR Lite v3 sensor, eliminating the need for expensive optical modules or deep-learning hardware. By analysing the geometric behaviour of laser reflections at varying incidence angles, the system can differentiate black ice from asphalt in real time without being affected by thermal sensitivity or lighting conditions. This makes the approach particularly effective for resource-limited environments or embedded systems where computational and installation constraints are critical. Furthermore, the integration of explainable AI frameworks into these models has enabled more transparent decision-making, which is crucial for practical deployment in intelligent transportation systems. These developments open the door to real-time, high-confidence black ice detection mechanisms that can be embedded into autonomous driving platforms or connected infrastructure, ultimately contributing to accident

prevention and the advancement of road safety technologies. Building on these developments, recent studies have demonstrated how AI-based models can significantly enhance LiDAR-driven surface analysis. For example, BlackIceNet applied an explainable multimodal framework combining LiDAR intensity, temperature, and camera imagery, achieving superior detection reliability under low-visibility conditions. Similarly, Lee et al. utilized convolutional neural networks (CNNs) to classify icy and non-icy surfaces from sensor data, improving real-time responsiveness for automated vehicles. Furthermore, fuzzy logic–based models have shown strong adaptability by integrating LiDAR intensity with environmental parameters such as humidity and surface temperature, reaching up to 87% detection accuracy under Arctic conditions. Integrating these AI techniques into the proposed method could enable adaptive thresholding, noise filtering, and context-aware decision-making—ultimately advancing the robustness and scalability of black ice detection systems in intelligent transportation infrastructure.

Fig. 1: Black Ice on Asphalt.

2.2. Lidar sensor

LiDAR sensors function by detecting objects and measuring distances through the use of laser light. This remote sensing technology relies on emitting pulses of light and analyzing the time it takes for each pulse to return after reflecting off a surface. By calculating the time of flight based on the known speed of light and the direction of emission, the sensor can determine the exact distance to an object. This process allows for accurate spatial recognition, including the identification of an object's shape, position, and movement. In this study, we apply this principle to construct three-dimensional coordinates of road surfaces. The technique involves sequential signal acquisition and real-time data processing, enabling detailed environmental mapping. Such capabilities make LiDAR an effective tool for various applications, from autonomous navigation to industrial monitoring, where high-resolution and precise spatial awareness are required.

Fig. 2: Lidar Lite v3 Module.

The reflective behavior of a surface can typically be categorized into three types: diffuse reflection, specular reflection, and retroreflection. In real-world scenarios, however, these characteristics often appear in combination rather than in isolation. Diffuse reflection is most commonly observed in rough or textured surfaces, where incident light is scattered uniformly in many directions. This uniform dispersion leads to a more consistent return signal to the LiDAR sensor, which can improve measurement reliability. In contrast, smooth surfaces may cause specular or retroreflective behavior, resulting in less predictable signal returns. Table 1 presents the measurement errors associated with various surface materials when scanned at a fixed angle. The results indicate that both the material type and the actual distance to the target influence the sensor's accuracy. While the Lidar Lite v3 demonstrates sufficient precision for controlled experiments, its ±1 cm error tolerance can lead to significant deviations under real-world conditions. Factors such as uneven road geometry, surface moisture, or varying ice thickness can alter the reflection path and introduce cumulative range errors. In dynamic environments, these variations may result in false readings or missed detections, particularly when the LiDAR operates near its minimum detection threshold. According to prior performance evaluations of compact LiDAR modules [5], range accuracy can degrade under high humidity or low-reflectivity surfaces, and similar robustness assessments in autonomous-vehicle contexts [17] emphasize the need for adaptive filtering and environmental calibration. To address these limitations, future implementations should employ sensor fusion strategies, combining LiDAR with complementary sensing modalities such as thermal or optical cameras, and incorporate real-time calibration routines to maintain measurement reliability across diverse road conditions.

Table 1: Measurement Error by Material Type Using Lidar Lite v3

Measurements Taken at 70° Substance	Measurement distance [cm]	A real distance [cm]	Error rate [%]
Ceramics	188.01	190	1.044
Tile	211.61	196	7.964
Wood	190.67	184	3.625
Concrete	166.56	171	2.556
Porcelain	183.83	184	0.092
Asphalt	168.49	170	0.888
Paving Stone	168.22	164	2.573
Grass	228.6	240	4.75
Cement	169.21	179	5.469
Sand	225.57	220	2.532

2.3. Distance estimation using lidar lite v3

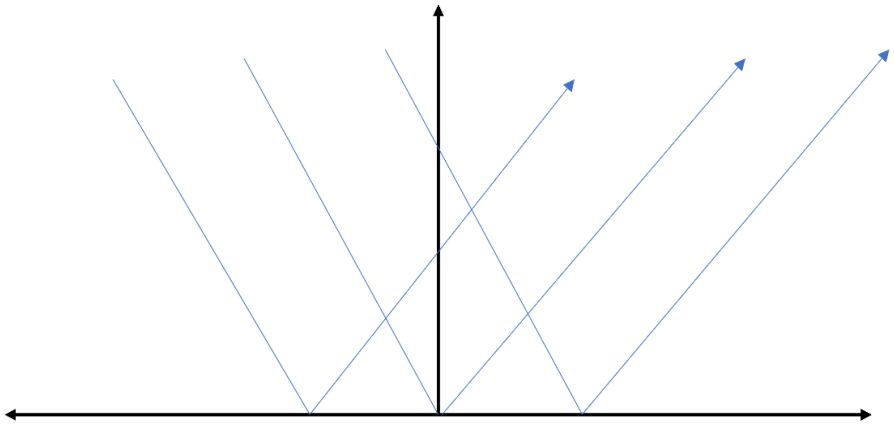

Fig. 3: Reflected Waves.

V = propagation speed of the laser (typically the speed of light in air).
f = frequency of the laser signal.
λ = wavelength of the laser signal.
D = distance to the target.
T = round-trip time of the laser pulse (ToF: time of flight).
α = Empirical calibration coefficient (unitless).

$$V = f \times \lambda \tag{1}$$

$$D = \alpha(V \times T) / 2 \tag{2}$$

After calibrating the sensor's light sensitivity, the LiDAR continuously emits a sequence of laser pulses toward the target surface. The reflected signals are compared with stored reference data to identify valid measurements, while correlation analysis is applied to reduce noise and ensure consistency in the received signals. This process repeats automatically until a reflection surpasses a predefined threshold, at which point the system calculates the distance using the time-of-flight (ToF) principle. To improve accuracy, a calibration coefficient (α) is applied to correct for minor deviations caused by environmental or sensor factors. Once the distance value is obtained, it is immediately output, and the measurement cycle restarts for continuous, real-time operation. During reflection, the frequency and wavelength of the transmitted wave remain constant, but the direction of the reflected wave changes depending on the surface angle and texture, as described in Equation (2).

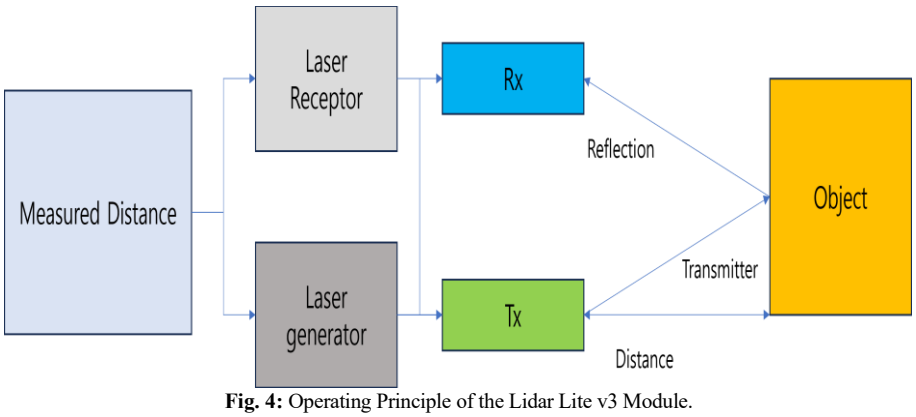

Fig. 4: Operating Principle of the Lidar Lite v3 Module.

2.4. Black ice discrimination based on reflective properties

As shown in Figure 4, the Lidar Lite v3 sensor can detect the presence of black ice by measuring subtle changes in surface distance and reflection patterns. By analyzing laser returns from the ground, the sensor enables the identification of icy conditions that are otherwise difficult

to observe visually. In this study, temperature and angle were systematically varied to evaluate how these factors influence measurement values. This approach allows for distinguishing black ice from regular asphalt surfaces based on reflective properties and surface response. Since black ice tends to reflect light more uniformly than textured surfaces like asphalt, the resulting data can also be used to estimate surface glossiness. Additionally, incorporating information about surface roughness further improves detection accuracy by compensating for irregular reflectance behavior.

3. Research Results

3.1. Temperature simulation results

In this section, an analysis of the distance data returned by the lidar sensor is conducted in the critical temperature range where black ice forms. All experiments were conducted with a 90-degree angle of incidence, a distance of 1.60 meters from the sensor to the road surface, and a fixed ice thickness of 3 centimeters. The following Table 2 presents a comparison of the measurements from the temperature-based simulation to those of normal asphalt and black ice as a function of temperature.

Table 2: Difference from Actual Distance by Temperature

Temperature [C]	Asphalt [m]	Blackice [m]	Difference [m]
-4	1.668	1.637	0.071
-3	1.546	1.516	0.028
-2	1.648	1.618	0.029
-1	1.606	1.576	0.030
0	1.672	1.641	0.031
1	1.501	1.471	0.027
2	1.590	1.560	0.027
3	1.539	1.509	0.026
4	1.745	1.715	0.026

Although Table 2 shows only minimal variation in distance, this is primarily due to the sensor's low sensitivity to thermal variation and the optical transparency of ice, which reduces LiDAR reflectivity changes. Moreover, environmental factors such as humidity and frost accumulation can further obscure temperature-based distinctions, limiting the reliability of temperature-driven detection. A variation of approximately 0.030 meters. This provides experimental evidence that the actual measurements are not significantly affected by temperature variations around the freezing point. Figure 5 provides a visual representation of the measured distance of asphalt and black ice along the temperature axis. It is evident that both curves are situated within the same axis range. The graph illustrates that the asphalt curve lies above the black ice curve over the entire temperature range.

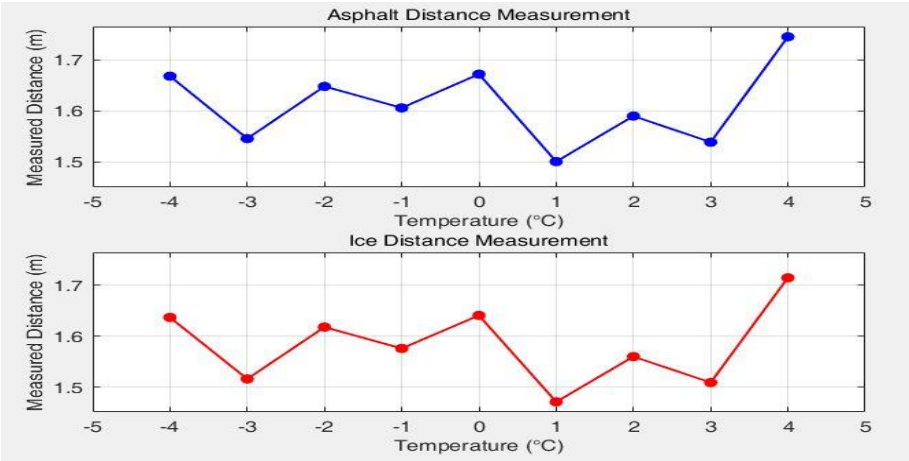

Fig. 5: Graph of Actual Distance Comparison by Temperature.

Figure 5. A comparison of the measured LiDAR distances for asphalt (blue) and black ice (red) surfaces has been conducted across a temperature range from -4 °C to +4 °C. The analysis of both datasets indicates that they demonstrate nearly parallel behaviour, with variations in distance measurement within a margin of error of ±1 cm. This finding suggests that variations in temperature do not exert a significant influence on the accuracy of LiDAR detection. The slightly lower curve for black ice is indicative of the optical transparency and thickness effects of the ice layer.

3.2. Angle simulation results

The angular simulation was utilized to analyze the effect of modifying the laser incidence angle, denoted by θ, on the ranging process. The distance from the sensor to the road surface, the thickness of the ice, and the surrounding environment were held constant, with the angle of incidence, designated as θ, varying in incremental steps. The distance measured by the sensor is calculated based on the time required for the D laser to initiate and complete its cycle, with the resulting angle designated as θ. Initially, the angle is transformed into radians. The results of the simulation are shown in Table 3.

$$\text{Horizontal Distance} = HD \tag{3}$$

$$HD = D \times \cos(\theta) \tag{4}$$

Table 3: Difference from Actual Distance by Incidence Angle

Incidence angle [θ]	Asphalt [m]	Blackic e[m]	Difference [m]
0	1.748	1.717	0.031
15	1.812	1.782	0.030
30	2.021	1.987	0.034
45	2.475	2.434	0.041
60	3.122	2.912	0.210
70	4.801	3.678	1.123
80	7.190	5.081	2.119

As demonstrated in Figure 6, the geometric configuration employed in the angular simulation corresponds directly to the distance variations presented in Table 3. The LiDAR module (positioned on the left) emits a laser beam (solid green line) towards the road surface at an incidence angle of θ > 60°, where the beam sequentially strikes two adjacent materials – asphalt (dark grey) and black ice (light blue). At these higher angles, the smooth ice surface exhibits strong specular reflection, as indicated by the dashed line, causing the reflected beam to deviate away from the receiver. This behaviour is evidenced by the sharp increase in the measured distance difference (ΔD) as shown in Table 3, where ΔD rises from 0.041 m at 45° to 2.119 m at 80°. Figure 6 provides a visual demonstration of how the angular geometry of reflection underpins the numerical divergence observed in Table 3, thereby confirming that high-angle specular reflection from black ice reduces return intensity and causes the LiDAR to register a shorter effective range than on asphalt.

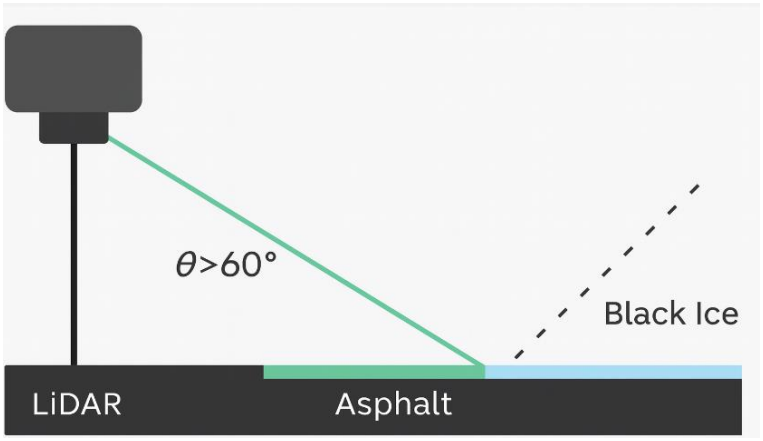

Fig. 6: Laser Reflection Trajectory at 45° Angle.

3.3. Advanced angular reflectance profiling for black ice discrimination

As illustrated in Figure 7, the distance difference between asphalt and black ice is measured continuously from 0° to 80° incidence angle. At temperatures below 50°, the standard deviation of the distance (ΔD) remains at a few centimeters and constitutes approximately 2% of the total measured distance, making it barely distinguishable from the sensor error. However, at 60°, the change rate (ΔD) increases sharply to approximately 0.2 m, and at 80°, it exhibits a pronounced increase to more than 2 m. At low angles, only minor thickness offsets appear, but at high angles (> 60°), specular reflection dominates, reducing the return intensity and causing the LiDAR to underestimate the actual range. This behavior validates the ΔD growth shown in Figure 7 and Table 3, demonstrating the effectiveness of angular profiling for black-ice identification. This determination can be made by adjusting the angle of incidence, obviating the necessity for additional video or thermal sensors. In summary, the incorporation of a tilt scan capacity of 60° or greater within an automotive LiDAR system enables the implementation of a system capable of instantaneously detecting and alerting drivers to the presence of black ice on the road, irrespective of variations in temperature and humidity.

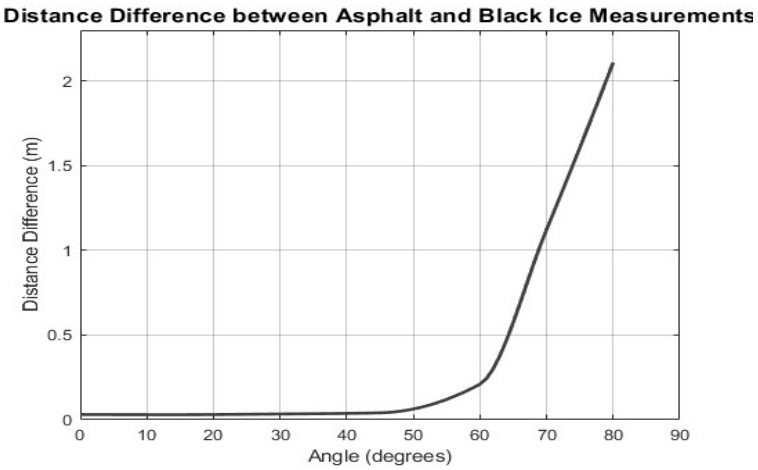

Fig. 7: Angles Difference between Asphalt and Black ice Measurements.

4. Conclusion

This study evaluated the effectiveness of the LIDAR Lite v3 sensor in detecting black ice by comparing surface reflectivity patterns of asphalt and ice under varying thermal and angular conditions. The experimental results demonstrated that while thermal variations between black ice and asphalt produced only marginal differences due to the sensor's limited responsiveness to temperature shifts, changes in the angle of incidence yielded significantly more pronounced effects. In particular, altering the laser beam's angle between 0° and 90° enabled consistent differentiation in reflectance characteristics, suggesting that angular profiling is a more viable strategy for practical detection. These insights highlight the limitations of relying solely on temperature-based indicators and support a shift toward geometric and structural reflectance cues in surface condition analysis. To enhance the reliability and scope of such detection systems, it is advisable to integrate additional sensing modalities such as thermal infrared imaging, multispectral or hyperspectral cameras, and machine learning classifiers. The incorporation of supplementary environmental variables like ambient humidity, road surface irregularity, and surface gloss can further refine the system's accuracy and reduce misclassification risks, especially in suboptimal lighting or weather conditions. To transition from controlled experiments to field-ready systems, comprehensive validation must be conducted under real-world scenarios including a range of road materials, traffic densities, and meteorological conditions. Furthermore, advancements in embedded AI and edge computing architectures provide new opportunities for developing fast-response black ice detection platforms that operate autonomously and communicate wirelessly with transportation infrastructure. Although the proposed approach has proven effective under controlled laboratory settings, scaling it for real-world deployment in advanced driver-assistance systems (ADAS) and road infrastructure requires careful consideration of environmental and operational factors. Large-scale implementations would necessitate cost-efficient LiDAR node networks, equipped with protective housings and adaptive calibration to withstand variable weather, road vibrations, and contamination such as dust or frost. Furthermore, system-wide synchronization and data fusion among multiple sensing units would be essential to maintain measurement integrity across extended road segments. Previous experimental field validations have shown that maintaining detection reliability under diverse meteorological conditions—including heavy fog, precipitation, and fluctuating surface temperatures—remains a key challenge for practical adoption. Addressing these scalability aspects will be crucial before transitioning from prototype to full-scale intelligent road monitoring systems. Future work should prioritize the design of intelligent sensor fusion frameworks and the curation of large annotated datasets to support model training and validation. These developments will be instrumental in building robust, scalable systems for intelligent transportation and roadway safety.

Acknowledgement

Research was conducted through the Hanseo University on-campus research support project.

References

[1] Hyung Gyun Kim, "A Black Ice Detection Method Using Infrared Camera and YOLO," Journal of the Korea Institute of Information and Communication Engineering Journal of the Korea Telecommunications Society Vol.25, No.12:1874~1881, Dec.2021.

[2] Golam Mohtasin, Hyoung-Kyu Song, Anjith George, and Seong-Whan Lee, "BlackIceNet: Explainable AI-Enhanced Multimodal for Black Ice Detection to Prevent Accident in Intelligent Vehicles," *IEEE Internet of Things Journal*, vol. 12, no. 6, pp. 5123–5135, Jun. 2025. https://doi.org/10.1109/JIOT.2025.3530565.

[3] Dong-Han Lee, "A Study on the Design of Forest IoT Network with Edge Computing,"Journal of KIIT. Vol. 16, No10, pp.101-109, Oct.31,2018.pISSN 1598-8619, eISSN 2093-7571. https://doi.org/10.14801/jkiit.2018.16.10.101.

[4] Kim, Seung-Jun, Won-Sub Yoon, and Yeon-Kyu Kim., "Characteristics of Black Ice Using Thermal Imaging Camera"Journal of the Korean Society of Industry Convergence 24.6_2(2021): 873-882.

[5] E. Ayala, J. Sotamba, B. Carpio and O. Escandón"Lidar Lite v3 Module Performance Evaluation" 978-1-5386-6657-9/18/$31.00.

[6] Lee, HoJun, et al. "Black ice detection using CNN for the Prevention of Accidents in Automated Vehicle." *2020 International Conference on Computational Science and Computational Intelligence (CSCI)*. IEEE, 2020. https://doi.org/10.1109/CSCI51800.2020.00222.

[7] LIU, Tieming, et al. Prototype decision support system for black ice detection and road closure control. *IEEE Intelligent transportation systems magazine*, 2017, 9.2: 91-102. https://doi.org/10.1109/MITS.2017.2666587.

[8] Ma, Xinxu, and Chi Ruan. "Method for black ice detection on roads using tri-wavelength backscattering measurements." Applied optics 59.24 (2020): 7242-7246. https://doi.org/10.1364/AO.398772.

[9] Lee, Hojun, et al. "The detection of black ice accidents for preventative automated vehicles using convolutional neural networks." *Electronics* 9.12 (2020): 2178. https://doi.org/10.3390/electronics9122178.

[10] *M. Loetscher, N. Baumann, E. Ghignone, A. Ronco, and M. Magno, "Assessing the robustness of LiDAR, Radar and depth cameras against ill-reflecting surfaces in autonomous vehicles: an experimental study," arXiv preprint, arXiv:2309.10504, 2023.Ruiz-Llata et al. (2018)* introduced diffuse reflectance near-infrared spectroscopy for proactive road condition assessment, including ice presence ahead of moving vehicles. https://doi.org/10.1109/WF-IoT58464.2023.10539485.

[11] M. Ruiz-Llata, et al., "LiDAR design for road condition measurement ahead of a moving vehicle using near-infrared diffuse reflectance spectroscopy," *Sensors and Actuators A: Physical*, vol. 274, pp. 94–103, 2018.

[12] N. Certad, W. Morales-Alvarez, and C. Olaverri-Monreal, "Road markings segmentation from LiDAR point clouds using reflectivity information," *arXiv preprint*, arXiv:2211.01105, 2022. https://doi.org/10.1109/ICVES56941.2022.9986939.

[13] X. Ma and C. Ruan, "Method for black ice detection on roads using tri-wavelength backscattering measurements," *Applied Optics*, vol. 59, no. 24, pp. 7242–7246, 2020. https://doi.org/10.1364/AO.398772.

[14] S.-B. Hong and H.-S. Yun, "Predicting black ice-related accidents with probabilistic modeling using GIS-based Monte Carlo simulation," *PLOS ONE*, vol. 19, no. 5, e0303605, 2024. https://doi.org/10.1371/journal.pone.0303605.

[15] Y. Kim, J. Park, and D. Lee, "Development of LiDAR and thermal imaging-based response technology for black ice detection," *Sensors*, vol. 25, no. 10, pp. 1210–1224, 2025.

[16] S.-I. Kang and Y.-S. Shin, "Development of detection and prediction response technology for black ice using multi-modal imaging," *Engineering Proceedings*, vol. 102, no. 1, art. 8, Jul. 2025, https://doi.org/10.3390/engproc2025102008.

[17] M. Loetscher, N. Baumann, E. Ghignone, A. Ronco, and M. Magno, "Assessing the robustness of LiDAR, radar and depth cameras against ill-reflecting surfaces in autonomous vehicles: an experimental study," *arXiv preprint*, arXiv:2309.10504, 2023. https://doi.org/10.1109/WF-IoT58464.2023.10539485.

[1] A. S. Author et al., "Fuzzy logic-based slipperiness detection integrating LiDAR intensity with environmental parameters," *Frontiers in Artificial Intelligence*, 2025, testing accuracy 87 % under Arctic conditions.